BonnMu: A Sequence-Indexed Resource of Transposon-Induced Maize Mutations for Functional Genomics Studies[1[OPEN]]

Caroline Marcon,[a,2,3] Lena Altrogge,[b,2] Yan Naing Win,[a] Tyll Stöcker,[b] Jack M. Gardiner,[c] John L. Portwood II,[d] Nina Opitz,[a,4] Annika Kortz,[a] Jutta A. Baldauf,[a] Charles T. Hunter,[e,5] Donald R. McCarty,[e] Karen E. Koch,[e] Heiko Schoof,[b,3] and Frank Hochholdinger[a,3,6]

[a]Institute of Crop Science and Resource Conservation, Crop Functional Genomics, University of Bonn, 53113 Bonn, Germany
[b]Institute of Crop Science and Resource Conservation, Crop Bioinformatics, University of Bonn, 53115 Bonn, Germany
[c]Division of Animal Sciences, University of Missouri, Columbia, Missouri 65211
[d]USDA-ARS Corn Insects and Crop Genetics Research Unit, Ames, Iowa 50011
[e]Horticultural Sciences Department, Plant Molecular and Cellular Biology Program, Genetics Institute, University of Florida, Gainesville, Florida 32611

ORCID IDs: 0000-0001-6699-9441 (C.M.); 0000-0002-6871-235X (L.A.); 0000-0002-4043-5194 (Y.N.W.); 0000-0001-7184-9472 (T.S.); 0000-0002-1804-0110 (J.M.G.); 0000-0002-6339-0881 (J.L.P.); 0000-0003-0776-4890 (N.O.); 0000-0002-1825-0660 (A.K.); 0000-0002-7286-0558 (J.A.B.); 0000-0002-2652-9485 (C.T.H.); 0000-0001-8694-5117 (D.R.M.); 0000-0003-1469-8799 (K.E.K.); 0000-0002-1527-3752 (H.S.); 0000-0002-5155-0884 (F.H.)

Sequence-indexed insertional libraries in maize (*Zea mays*) are fundamental resources for functional genetics studies. Here, we constructed a *Mutator* (*Mu*) insertional library in the B73 inbred background designated *BonnMu*. A total of 1,152 *Mu*-tagged F_2-families were sequenced using the *Mu*-seq approach. We detected 225,936 genomic *Mu* insertion sites and 41,086 high quality germinal *Mu* insertions covering 16,392 of the annotated maize genes (37% of the B73v4 genome). On average, each F_2-family of the *BonnMu* libraries captured 37 germinal *Mu* insertions in genes of the Filtered Gene Set (FGS). All *BonnMu* insertions and phenotypic seedling photographs of *Mu*-tagged F_2-families can be accessed via MaizeGDB.org. Downstream examination of 137,410 somatic and germinal insertion sites revealed that 50% of the tagged genes have a single hotspot, targeted by *Mu*. By comparing our *BonnMu* (B73) data to the *UniformMu* (W22) library, we identified conserved insertion hotspots between different genetic backgrounds. Finally, the vast majority of *BonnMu* and *UniformMu* transposons was inserted near the transcription start site of genes. Remarkably, 75% of all *BonnMu* insertions were in closer proximity to the transcription start site (distance: 542 bp) than to the start codon (distance: 704 bp), which corresponds to open chromatin, especially in the 5′ region of genes. Our European sequence-indexed library of *Mu* insertions provides an important resource for functional genetics studies of maize.

The genome of the maize (*Zea mays*) inbred line B73v4 is predicted to contain 44,117 genes, including 39,179 high confidence protein encoding gene models and 4,938 genes encoding for large intergenic noncoding RNAs, transfer RNAs, and microRNAs (Jiao et al., 2017). To date only a few hundred of these genes have been functionally characterized (Schnable and Freeling, 2011). The identification of specific mutants in forward genetic screens and the subsequent cloning of the underlying genes has been the method of choice to determine gene functions for several decades (Candela and Hake, 2008). Until now, reverse genetics using specific gene sequences as a starting point for the identification of the corresponding mutants (Candela and Hake, 2008) has mainly been used to independently validate candidate genes identified by forward genetics experiments (e.g. Hochholdinger et al., 2008; Nestler et al., 2014). Nevertheless, reverse genetics has also been successfully applied to identify developmental mutants of genes without prior knowledge of their phenotype (Xu et al., 2015). Genome-wide insertional mutagenesis is a tool to create loss-of-function mutations for virtually all genes in a genome by the insertion of DNA into the gene of interest. Sequence-indexed collections of such mutants have been generated for Arabidopsis (*Arabidopsis thaliana*; Alonso et al., 2003), rice (*Oryza sativa*; Hirochika et al., 2004), and maize (Fernandes et al., 2004; McCarty et al., 2005; Liang et al., 2019).

Endogenous transposons or transposable elements (TEs) are mobile DNA sequences initially discovered in maize by McClintock (1951). Once activated, a transposon can move from one location in the genome to another, thereby disrupting genes. The two major classes of transposons are class I retrotransposons and class II DNA transposons. The main difference between these classes is their mode of transposition. Class I retrotransposons first require transcription of their DNA to an RNA intermediate, which is then reversely transcribed into DNA, before it is reinserted into a new

genomic location (for review, see Feschotte et al., 2002). This mechanism is catalyzed by a reverse transcriptase. In contrast, the TE itself is the transposition intermediate for class II DNA transposons. Both classes have in common that they consist of autonomous and nonautonomous TEs. Autonomous TEs can transpose by themselves, because they encode a transposase, whereas nonautonomous TEs require another autonomous transposon to move. Class I transposons are predominantly intergenic, contributing to plant genome size (Bennetzen, 2000). In contrast, class II TEs insert preferentially in and around genes (Dietrich et al., 2002; Fernandes et al., 2004; Settles et al., 2004), which is a prerequisite for genome-wide insertional mutagenesis screens.

The most active class II transposon family in maize is the family of *Mutator* (*Mu*) elements (Lisch, 2002). Discovered by Robertson (1978), *MuDR,* an autonomous TE, controls the transposition of itself and 16 classes of nonautonomous *Mu* elements (Lisch, 2015). All *Mu* transposons share highly conserved 215-bp terminal inverted repeats (TIRs) at both ends of the element and upon insertion they generate 9-bp target site duplications directly flanking the *Mu* transposon sequences. For untargeted insertional mutagenesis, *Mu* exhibits a number of advantages over other maize class II transposon families, such as Activator/Dissociation (*Ac*/*Ds*) or Enhancer/Suppressor-mutator (*En*/*Spm*), including its high transposition rate and high-copy number (Chandler and Hardeman, 1992). While *Ac*/*Ds* transposons exhibit a preference for regional mutagenesis (i.e. transposition into closely linked genes; Brutnell, 2002), *Mu* elements randomly target genes throughout the maize genome (Lisch, 2002). As such, *Mu* insertion site frequencies strongly correlate with gene density (Liu et al., 2009; Schnable et al., 2009; Springer et al., 2018).

In the past, adapter-mediated (Frey et al., 1998) and thermal asymmetric interlaced-PCR (Liu and Whittier, 1995) have been used to amplify *Mu*-flanking fragments for sequencing. The presence of highly conserved TIR sequences at both ends of the transposons is ideally suited to design *Mu*-specific primers used in thermal asymmetric interlaced-PCR. This PCR technique combines nested TIR-specific primers and degenerative arbitrary primers to amplify sequences neighboring known sequences by using high and low annealing temperature cycles (Settles et al., 2004). More recently, high-throughput next generation sequencing enables efficient, reproducible, and sequence-based identification and mapping of transposon insertion sites in maize (McCarty et al., 2013; Liu et al., 2016; Liang et al., 2019).

Thus far, several transposon-tagged maize populations have been generated using the *Mu* transposon system (Fernandes et al., 2004; Stern et al., 2004; McCarty et al., 2005; McCarty et al., 2013; Liang et al., 2019). Nevertheless, to date only about 52% of the annotated maize gene models (Liang et al., 2019) have mapped *Mu* insertions. Among these collections, the insertion-tagged *UniformMu* population (McCarty et al., 2005) has been developed by backcrossing an active *MuDR* element eight times into the genetically uniform inbred line W22. A genetically uniform genetic inbred background is one key feature of the *UniformMu* resource, because it allows to distinguish between parental and newly created mutations. Therefore, a uniform background aids to identification of insertions related to new phenotypes (McCarty et al., 2005). A large set of more than 14,000 *UniformMu* lines are publicly available (Liu et al., 2016). Another *Mu* insertional library, called *ChinaMu*, has been generated by crossing a *Mu*-starter line to the inbred line B73 (Liang et al., 2019). The *Mu*-tagged sequences of 2,581 F_2-*Mu* lines were isolated by a *Mu* tag enrichment approach and sequenced by high-throughput sequencing.

Here we used the *Mutator*-seq approach (*Mu*-seq; McCarty et al., 2013; Liu et al., 2016) to construct multiplexed sequencing libraries in the inbred line B73 that guarantees unbiased coverage of mutations in the maize genome. The *Mu*-seq reverse genetics approach enables the identification of F_2-families carrying transposon insertions in genes of interest in a sequence-indexed transposon tagged population. These newly identified transposon induced mutations can be used for subsequent molecular and genetic analyses. Furthermore, this European database (*BonnMu*) of sequence-indexed *Mu* transposon insertion sites in B73 complements the *UniformMu* and *ChinaMu* resources and allows for forward and reverse genetics experiments. Besides the sequence-indexed *Mu* insertional libraries from North America (*UniformMu*) and Asia (*ChinaMu*), our resource of transposon induced

[1]This work was supported by the Deutsche Forschungsgemeinschaft (grant no. MA 8427/1–1 to C.M.), the Bundesministerium für Bildung und Forschung (grant no. 031 B195C to F.H.), and the United States Department Agriculture, Agricultural Research Service to J.L.P. and C.T.H.

[2]These authors contributed equally to this article.

[3]Senior authors.

[4]Present address: Federal Ministry of Food and Agriculture, 53123 Bonn, Germany

[5]Present address: USDA-ARS Chemistry Research Unit, Gainesville, FL 32608

[6]Author for contact: hochholdinger@uni-bonn.de.

The author responsible for distribution of materials integral to the findings presented in this article in accordance with the policy described in the Instructions for Authors (www.plantphysiol.org) is: Caroline Marcon (marcon@uni-bonn.de).

C.M. and L.A. interpreted the data and drafted the article; C.M. and F.H. conceived the research; C.M., Y.N.W., N.O., and A.K. generated the *Mu*-seq libraries; C.M. and Y.N.W. phenotyped the *Mu*-seq families and prepared seedling photos for public access via MaizeGDB.org; L.A., T.S., and H.S. conceived and carried out the bioinformatics analyses; J.M.G. and J.L.P. curated insertions and phenotypes of the *Mu*-tagged families at MaizeGDB.org; C.T.H., D.R.M., and K.E.K. provided W22 datasets and participated in data interpretation; J.A.B. was involved in statistical analysis; H.S. and F.H. participated in data interpretation, coordinated the study, and helped to draft the article; all authors approved the final draft of the article.

[OPEN]Articles can be viewed without a subscription.

www.plantphysiol.org/cgi/doi/10.1104/pp.20.00478

Table 1. Mu-*seq library alignment statistics*

Statistical Analysis	*Mu*-seq 1	*Mu*-seq 2	Combined
Raw read pairs	89,833,184	55,248,154	–
Read pairs after trimming[a]	65,773,604	43,651,352	–
Average alignment rate	89%	83%	–
Remaining read pairs after removing duplicate reads[b]	23,251,540	18,785,728	–
Union (somatic and germinal insertions)[c]			
Insertion sites	135,108	112,205	225,936
Insertion sites in FGS genes	81,698	68,413	137,410
Insertion sites in exons of FGS genes	66,270	55,221	110,730
Insertion sites in cds of FGS genes	22,743	19,743	40,140
Insertion sites in 5′ UTR of FGS genes	46,362	37,945	75,201
Insertion sites in 3′ UTR of FGS genes	4,085	3,361	7,125
Insertion sites in introns of FGS genes	14,586	12,404	25,203
Insertion sites upstream of FGS genes (≤ 500 bp)	23,268	19,411	38,609
Intergenic insertion sites	53,410	43,792	88,562
Mu-tagged FGS genes	19,162	17,923	22,362
Intersection (germinal insertions)[d]			
Insertion sites	43,225	24,234	66,750
Insertion sites in noncoding DNA	16,462	9,323	25,664
Insertions sites in FGS genes	26,762	14,912	41,086
Mu-tagged FGS genes	13,590	9,538	16,392
Mu-tagged FGS genes, affected in their cds	5,605	3,487	7,582

[a]*Mu*-seq reads were trimmed and aligned to the B73v4 genome as described in the "Materials and Methods" section. [b]Duplicate reads were removed as described in the "Materials and Methods" section. [c]All insertion sites identified in any of the samples. Insertion sites were identified as described in the "Materials and Methods" section. [d]Insertion sites identified in only one row and one column sample, respectively.

mutations will offer easier access for European researchers but also for maize geneticists around the globe.

RESULTS

Mu-seq Library Alignment Statistics of *BonnMu*

To generate a sequence-indexed collection of transposon tagged maize mutants, the *Mu*-seq protocol (McCarty et al., 2013; Liu et al., 2016) was applied to generate two libraries each containing 576 Mu active B73 F_2-families (*BonnMu*) of maize. These 1,152 mutagenized F_2-families were pooled according to a 24 × 24 grid system per library (see "Materials and Methods"). Sequencing of the two libraries yielded 55 and 90 million raw read pairs (Table 1; Supplemental Dataset S1). Each *Mu*-seq library was parsed according to the individual 6-bp barcodes of the 48 multiplexed pools (Supplemental Table S1), resulting in an averaged output of 1,151,003 and 1,871,525 read pairs per pool (Supplemental Dataset S1). Downstream statistical analysis of the two *Mu*-seq libraries are summarized in Table 1. After U-adapter and TIR sequences were trimmed, 83% and 89% (Table 1) of the remaining reads (43 and 65 million) were aligned to the B73 Filtered Gene Set (FGS) AGPv4.36, containing 44,117 high confidence gene models. After duplicate read removal, 18 and 23 million read pairs remained and were used to identify genomic insertion sites, in (1) any of the 48 pools (somatic and germinal insertions, named union in Table 1) and (2) at intersections of one row and one column pool (germinal insertions, named intersection in Table 1). For insertion site identification, reads were counted in each of the 48 pools. Only insertion sites supported by at least four reads were used for further analyses. In total, 225,936 genomic insertion sites were detected in the two *Mu*-seq libraries (Table 1; Supplemental Dataset S2). Among those insertion sites, 61% (137,410 of 225,936 insertions) mapped to FGS genes, tagging in total 22,362 genes (Table 1). Thus, there were on average six somatic or germinal insertions per tagged FGS gene. Further parsing of insertion sites identified 110,730 insertion sites in exons of FGS genes, 40,140 of such sites in the coding sequence, 75,201 sites in 5′ untranslated region (UTR), 7,125 insertion sites in 3′ UTR, and 25,203 insertion sites in introns of FGS genes. In addition, 38,609 insertion sites ≤500 bp upstream of FGS genes and 88,562 intergenic insertions were detected (Table 1). Based on the genome annotation of AGPv4.36, insertion sites can be assigned to more than one feature (e.g. both the 5′ UTR and exonic region), within a gene. To calculate the number of insertion sites in introns, the union of insertion sites located in exons/coding sequence (cds) and UTRs was subtracted from the number of insertion sites in FGS genes. Therefore, the number of insertion sites located in introns cannot be recalculated from Table 1.

Finally, to only consider heritable (germinal) insertions the information from the different pools was combined to track down *Mu*-tagged genes in specific F_2-families. Each F_2-family is represented by the intersection of one column and one row pool (according to the 24 × 24 grid system; Supplemental Table S1). By that criterion, we identified 66,750 germinal insertion sites in the two *Mu*-seq libraries, of which 38% (25,664

of 66,750) mapped to noncoding DNA (Table 1). The remaining 62% (41,086 of 66,750) of the insertion sites were located in genes of the FGS (Table 1; Supplemental Dataset S3). On average, each F_2-family harbored 37 germinal insertions in FGS genes (Supplemental Tables S2 and S3; Supplemental Dataset S3). Furthermore, 46% of mutated FGS genes (7,582 of 16,392 FGS genes) contained insertions in coding sequences.

European-Based *BonnMu* Complements the North American *UniformMu* and the Asian *ChinaMu* Resource

Based on the analysis of two *Mu*-seq libraries in B73 (*BonnMu*), *Mu* insertions affected 16,392 of 44,117 (37%; Fig. 1A; Table 1) high-confidence gene models of maize. Of the 16,392 genes, 41% (6,763) were identified in F_2-families of both *Mu*-seq libraries, whereas 59% (9,656) of the genes were uniquely detected in one of the *Mu*-seq libraries (Fig. 1A). We observed a significantly higher overlap of *Mu*-tagged genes in both *Mu*-seq libraries than expected (2,938; Supplemental Table S4). This finding supports the notion that genes are not randomly targeted by *Mu* transposons, but that there is a preference for *Mu* tagging of specific genes.

The 16,392 genes of the *BonnMu* collection in the B73 background was compared with 16,090 *Mu*-tagged genes of the *UniformMu* resource in the W22 background (McCarty et al., 2013) and to 20,396 genes tagged in B73 in the *ChinaMu* dataset (Liang et al., 2019) and personal communication with R. Song). The three collections cover 57% (25,140 of 44,117) of the genes present in the B73 reference genome AGPv4.36 (Fig. 1B). A considerable proportion of *Mu*-tagged genes, that is, 42% (10,623 of 25,140) were hit in all three collections. This number of overlapping genes was significantly higher than expected by pure chance (2,724; Supplemental Table S4), suggesting that at least some genes are preferentially targeted by *Mu* insertions.

BonnMu insertions can be browsed at the MaizeGDB Web site (https://www.maizegdb.org; Portwood et al., 2019) as previously described for the *UniformMu* database (Liu et al., 2016). A unique feature of *BonnMu* is that photos of seedling phenotypes of segregating F_2-families are linked to the database entries of each transposon insertion. To access and visualize B73 insertions in maizegdb.org, a gene model identifier is needed for the genome browser view. When "select track" and "Bonn*Mu*" are clicked, insertion sites become visible in the locus. Clicking on the insertion site links to the *Mu* insertion identifiers (e.g. *BonnMu*0000812) and the respective F_2-*Mu*-seq family (e.g. *BonnMu*-2-A-0596) and its respective phenotype 10 d after germination. Among the analyzed F_2-families various leaf color mutants were identified such as albino (e.g. *BonnMu*-2-A-0784) or pale green (e.g. *BonnMu*-2-A-0784). The mutation rate, detected on the basis of albino and pale green leaf phenotype, was 13% (149 of 1,152 F_2-families). Furthermore, shoot gravitropism mutants (e.g. *BonnMu*-2-A-0596, *BonnMu*-2-A-0598) were identified.

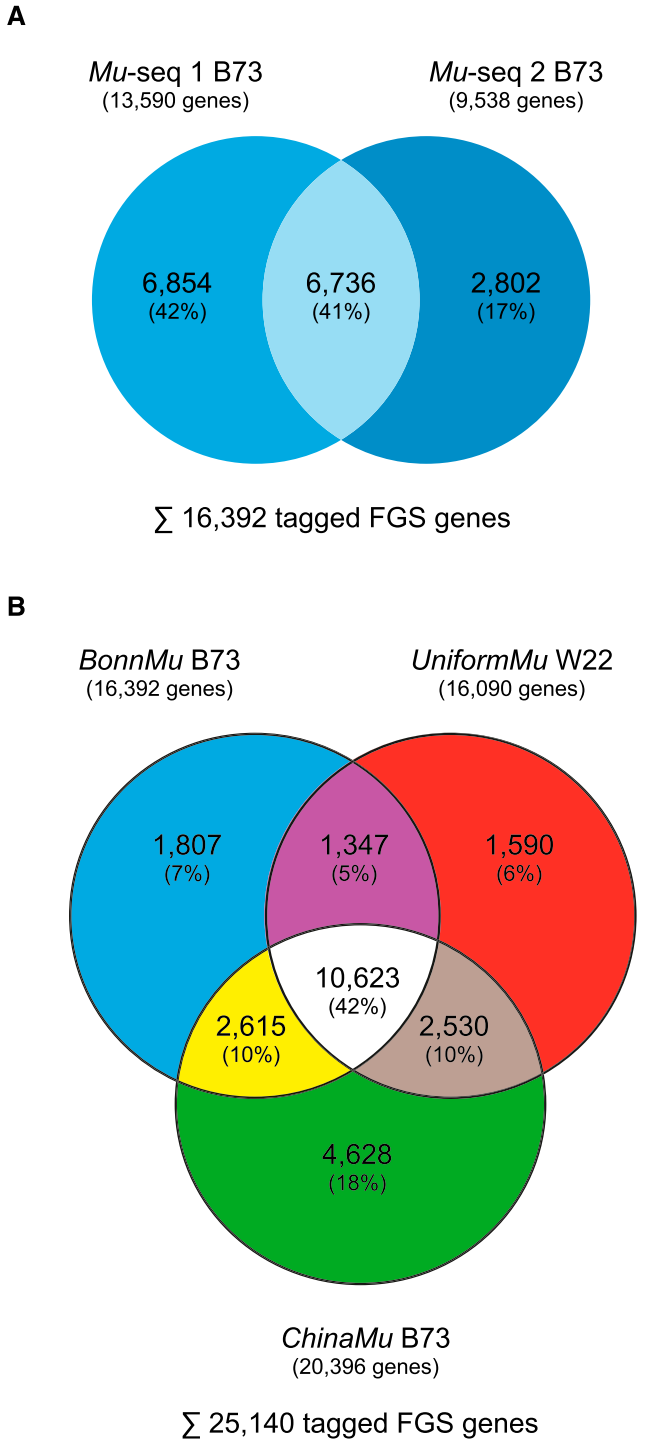

Figure 1. Overlap of FGS genes tagged by *Mu* transposon insertions. A, Tagged FGS genes among the two *Mu*-seq libraries in the B73 background. B, FGS genes with *Mu* insertions in the three available *Mu*-tagged resources in the B73 (blue, *BonnMu*; green, *ChinaMu*) and W22 inbred backgrounds (red, *UniformMu*).

The Number of *Mu* Insertions Correlates with Gene Length in a Size-Dependent Manner

The present dataset contains 41,086 *Mu* insertions in 16,392 B73 high confidence gene models (Table 1; Supplemental Dataset S3). More specifically, 39% (6,455 of 16,392) of the high-confidence gene models were tagged by a unique insertion (Fig. 2A), whereas 61% (9,937 of 16,392) contained at least two *Mu* insertions. A similar distribution was observed when the 7,582 FGS genes harboring insertions in their cds (Table 1; Supplemental Dataset S3) were analyzed. Among those, 33% (2,535 of 7,582) had a unique insertion, whereas 67% (5,047 of 7,582) were tagged by at least two *Mu* insertions (Fig. 2A). An extreme example is a gene encoding an adaptor protein 4 (AP-4) complex subunit μ (Zm00001d002925), which harbored 33 independent insertions in its cds (Supplemental Dataset S3).

The length of the affected genes ranged between 72 bp and 195 kb (Fig. 2B; Supplemental Dataset S3). The three shortest genes (72 bp) encode transfer RNAs (Zm00001d006818, Zm00001d007104, and Zm00001d034123), whereas the largest gene of 195 kb (Zm00001d001010) represents a large intergenic noncoding RNA. We observed 882 tagged genes (5% of all 16,392 *Mu*-tagged FGS genes) in a size range of 72 to 999 bp (Fig. 2B). Then, the size and the number of tagged genes increased, with a peak of 2,548 affected genes (16%) having a size between 3 and 3.999 kb. After this peak the number of affected genes decreased, while their length increased. Overall, 12,510 tagged genes (76%) had a size between 72 bp and 6.999 kb, whereas only 3,882 genes (24%) were >7 kb. In contrast with the observed distribution of the 16,392 tagged genes according to their gene length, the size distribution of all 44,117 B73v4 high-confidence gene models differed. Although 47% of all B73v4 gene models had a size of <2 kb, only 18% of all *Mu*-tagged genes of the present dataset ranged in that size (Supplemental Fig. S1). In contrast, 53% of all B73v4 gene models had a length between 2 and 194.5 kb, whereas among all *Mu*-tagged genes 82% ranged between these lengths.

Next, we tested the hypothesis that the number of *Mu* insertions increased with the length of the affected genes. Although a strong linear correlation of insertion number with gene size was detected in the gene size range of 72 bp to 3.999 kb, there was no correlation with gene size for genes >4 kb (Fig. 2B). Hence, the calculated Pearson correlation over all groups of gene sizes revealed no correlation (r = 0.06; Fig. 2C). This abrupt transition in gene-size dependence at 4 kb was also detected in the W22 dataset (Supplemental Fig. S2; Supplemental Dataset S4). Due to the fact that a large subset of 48% affected genes (7,838 B73 and 7,790 W22 genes) have a size of <4 kb, the gene-size-dependent correlation is important to consider.

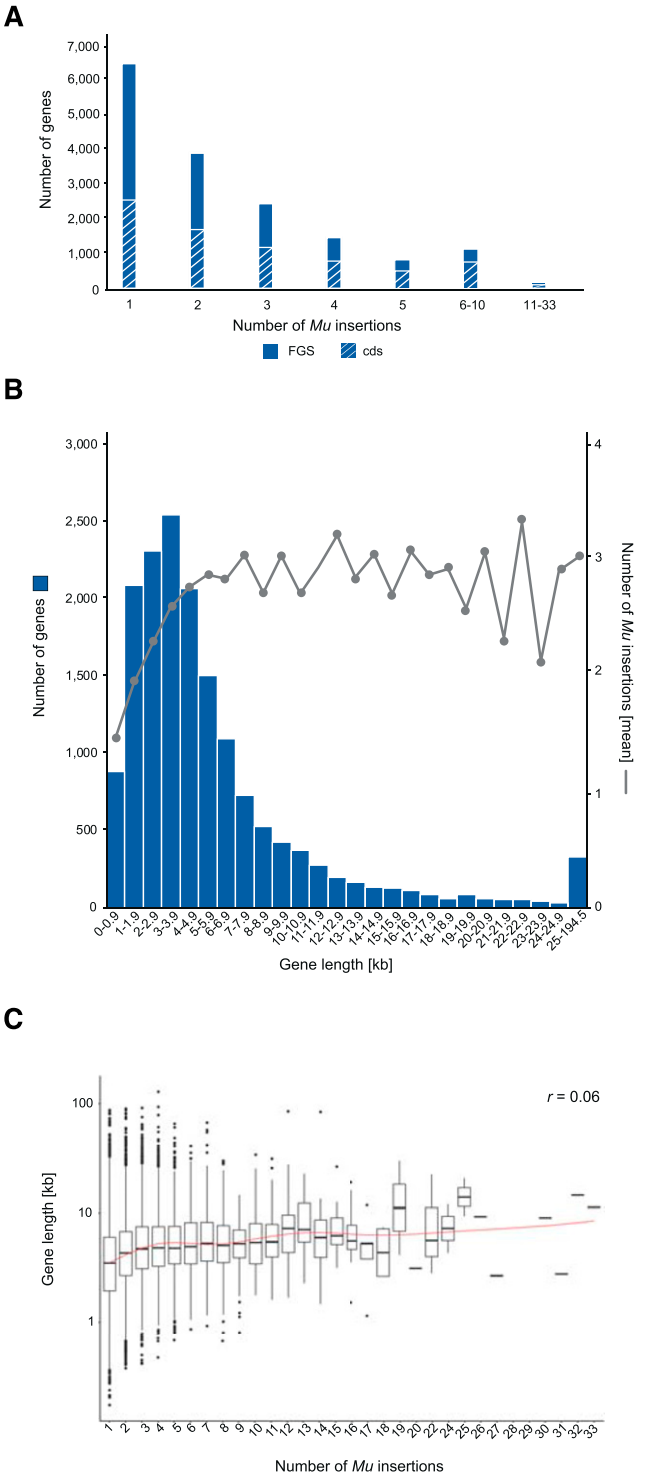

Figure 2. Number of *Mu* insertions and its correlation to the length of affected FGS genes of B73. A, Distribution and number of *Mu* insertions among 16,392 affected FGS genes and the subset of 7,582 genes harboring insertions in the cds of FGS genes. B, Number of tagged genes and associated mean number of *Mu* insertions plotted against the corresponding gene size. C, Length distribution of affected genes plotted against the individual number of *Mu* insertions (Pearson correlation coefficient, r = 0.06).

Table 2. *Number of expected and observed unique and overlapping bins (i.e. 200-bp sized regions of genes) targeted by* Mu *transposon insertions in B73 and W22*

Genotype	B73 YES	B73 NO	Total	Observed/Expected
W22 YES	293[a]	138	431	Observed
	50	381	–	Expected[b]
W22 NO	1,406	12,899	14,305	Observed
	1,649	12,656	–	Expected[b]
Total	1,699	13,037	14,736	–

[a]$P < 2.2\times e^{-16}$ (obtained from χ^2-testing). [b]Expected value of bins being hit in B73 and W22 was calculated as total number of bins identified in W22 (431)* total number of bins identified in B73 (1,699) / total number of bins (14,736).

Mu Insertion Hotspots Are Conserved Among Affected Genes of B73 and W22

Next, we investigated if *Mu* transposons show preferences regarding their insertion sites in the genes. Therefore, we examined all insertion sites in any of the samples, including somatic and germinal insertions of the present *BonnMu* datasest (Table 1; Supplemental Dataset S2). The majority of these insertion sites (61%; 137,410 of 225,936) was located in FGS genes. Each of the 22,362 *Mu*-tagged genes was divided into bins of 200 bp in size. Then, all insertion sites were sorted into the corresponding bins. Each bin with at least one insertion site was counted as a hotspot. In total, 38% (8,502 of 22,362 genes) of the *Mu*-tagged genes had one hotspot, which was predominantly targeted by the transposons (Supplemental Fig. S3A). The number of hotspots per affected gene ranged from 1 to 15, with a median number of two hotspots, independent of gene length (Supplemental Fig. S3B).

To investigate if insertion hotspots are conserved among affected genes of our *Mu*-seq repository in B73 and the *UniformMu* repository in the W22 genetic background, one exemplary W22 *Mu*-seq dataset (SRA accession SRP028545) was reanalyzed. A total of 558 identified insertion sites in W22 supported by at least two reads could be assigned to 423 FGS genes.

Among these 423 *Mu*-tagged genes in W22, 413 (98%) were also affected in B73. For the overlapping 413 genes a hotspot analysis was performed. Because we were interested in only conserved hotspots of new *Mu* insertion events, we first corrected the affected genes for endogenous *Mu* insertions that are present in the genomes of B73 and W22. About 40 canonical *Mu* elements exist in the two genomes (Springer et al., 2018; D. R. McCarty, personal communication; Supplemental Dataset S5). Due to the fact that such parental *Mu* elements are fixed in every B73/W22 plant, such elements account for a large proportion of reads. Hence, the endogenous elements could contribute to an apparent hotspot overlap between B73 and W22. After correcting for endogenous *Mu* elements, 22,348 B73 genes and 420 W22 genes remained. Among those, 412 genes overlapped between the two datasets and were divided into bins of 200 bp in length. Then, *Mu* transposon insertion sites identified in B73 and W22 were sorted into the corresponding bin. Out of 14,736 bins, 293 were targeted in both B73 and W22, 1,406 only in B73, 138 only in W22, and 12,899 in neither B73 nor W22 (Table 2). A χ^2-test was performed to test the hypothesis that there is an association between insertion sites in B73 and W22. The observed value of overlapping bins in both B73 and W22 (293) significantly exceeded the expected value of 50 bins, demonstrating that there are conserved insertion site hotspots in both genomes. This observation is exemplarily shown in Figure 3 for gene Zm00001d002371. Here, *Mu* transposon insertions were concentrated around two hotspots within that gene in B73 and one overlapping hotspot in W22.

Mu Transposons Preferentially Insert near the Transcription Start Site of Genes in B73 and W22

To investigate if *Mu* transposons show preferences regarding their insertion sites in genes, the union of all B73 *Mu* transposon insertion sites located in FGS genes was analyzed. A total of 110,730 of the insertion sites were located in exons of FGS genes (Table 1). Whereas 40,140 of the insertion sites were assigned to the cds of FGS genes, the majority of insertion sites (75,201) were located in the 5′ UTR of FGS genes.

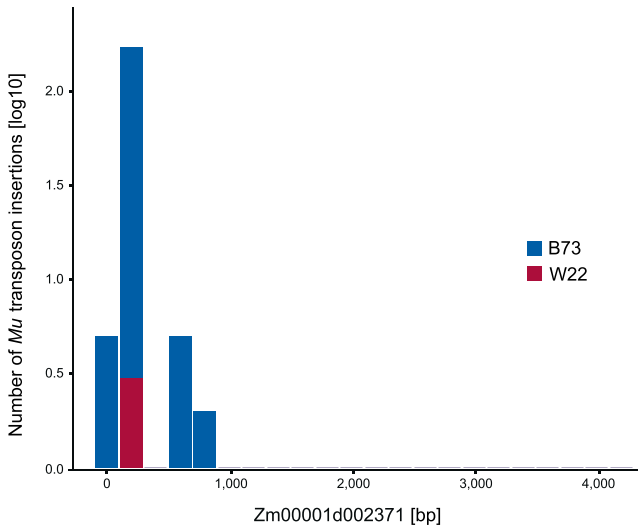

Figure 3. A *Mu* insertion hotspot in the representative gene Zm00001d002371 affected in the B73 and W22 genomes. The number of *Mu* insertions is plotted against location in Zm00001d002371.

To examine *Mu* transposon insertion site preferences in B73 compared with W22, for each affected FGS gene with annotated cds, the cds was divided into deciles. Subsequently, all insertion sites located in the cds of FGS genes were sorted into the corresponding cds decile. Insertion sites located up- or downstream of the cds were designated as insertions in the 5′ or 3′ UTR, respectively. The majority of *Mu* insertion sites was detected in the 5′ UTR and the first decile of the cds in both B73 (76%) and W22 (62%), with another smaller peak at the end of the cds (Fig. 4A). To account for the length of the FGS genes, all affected genes were sorted into gene sets based on their length (Supplemental Fig. S4A). Each of the sets (deciles) contained 2,152 affected B73 and either 42 or 43 affected W22 genes. Whereas in shorter genes of B73 (deciles 1% to 10%, and 11% to 20%) *Mu* insertions were evenly distributed among the gene, longer genes showed an insertion peak at the start region (i.e. the 5′ UTR and first 10% of the genes' cds; Fig. 4B). Another small peak of insertions was detected at the end of the cds (100%) of B73 genes.

Although the W22 dataset (SRP028545) only contained 423 genes, a similar preference of *Mu* insertions to target the 5′ UTR of the genes was observed (Fig. 4B). The observation that *Mu* insertions were evenly distributed among the gene of shorter genes, especially in B73, can be explained by the very short 5′ UTR of those genes. By comparing the length of the 5′ UTRs of each of the ten gene sets it became clear that the first two gene sets (1% to 10%, 135–1214 bp; 11% to 20%, 1215–1872 bp) had very short or even no 5′ UTRs (Supplemental Fig. S4B). Therefore, the absolute distance of insertions to the 5′ UTRs in those genes was small, even if the insertion was close to the 3′ end of the gene.

To verify if the insertion sites were located closer to the 5′ UTR start or closer to the start codon (ATG) of the affected genes, the distance (bp) from insertions inside or upstream of FGS genes to both the 5′ UTR start and cds start codon was calculated for the B73 dataset. The density plot (Fig. 5) represents only insertion sites located 500 bp upstream of the 5′ UTR to 2,000 bp downstream of the genes' start codon. Irrespective of this cutoff, the vast majority of 93% of all insertion sites are in the range of the above-mentioned distance to the 5′ UTR and 90% of all insertion sites are in such a distance to the cds. This result suggested that the majority of *Mu* insertion sites are close to the 5′ UTR and the cds start of the affected genes. This is also visible in the density plot (Fig. 5) where the majority of *Mu* insertion sites peaked in close proximity to the 5′ UTR and cds start. The slope of the curve revealed that the *Mu* transposon insertions are closer to the 5′ UTR than to the genes' start codon. Finally, 25% of all *Mu* insertion sites were located in close proximity to the 5′ UTR (46 bp) and to the cds start (111 bp; Fig. 5). When 50% of all insertion sites were considered, the distance was on average 135 bp to the 5′ UTR and 271 bp to the cds. Remarkably, 75% of all *Mu* insertion sites were located near the 5′ UTR (542 bp) and close to the start codon (704 bp) of the affected genes. In summary, this data revealed that the majority of *Mu* insertion sites are located closer to the 5′ UTR TSS than to the cds start of affected genes.

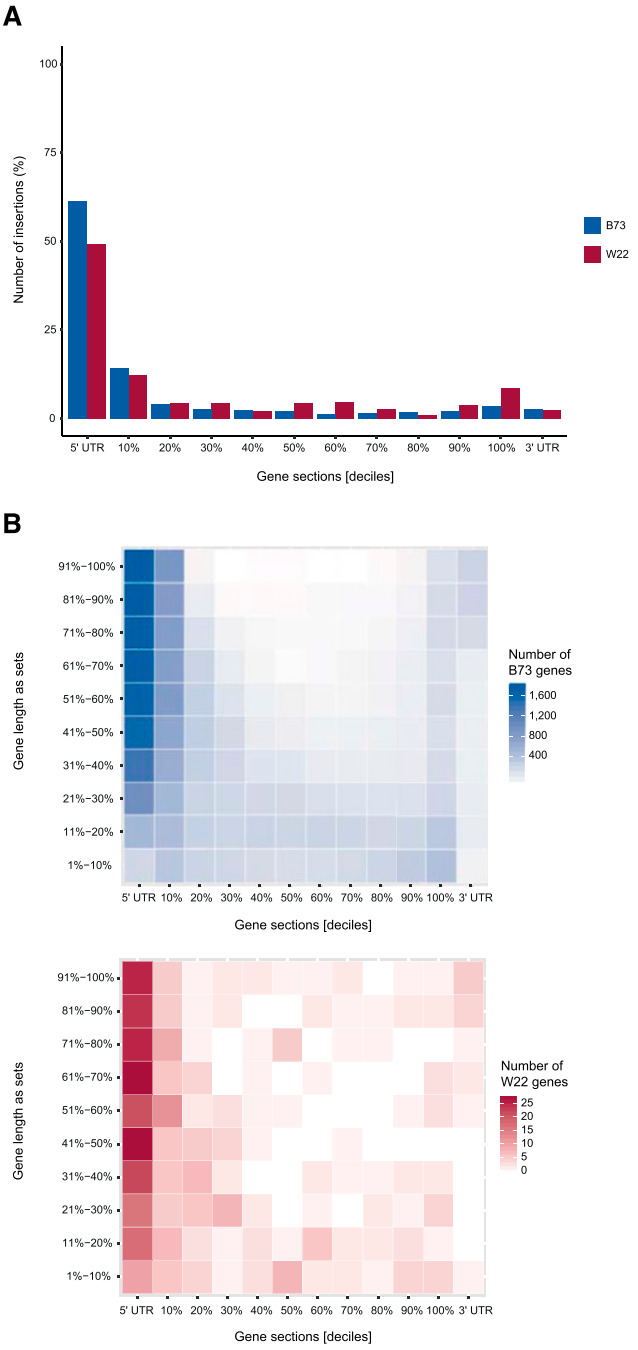

Figure 4. Distribution of *Mu* transposon insertion sites in FGS genes. A, Proportion of *Mu* insertions located in each decile of the cds, 5′ UTR, and 3′ UTR (B73, blue; W22, red). B, All FGS genes targeted by *Mu* transposons in B73 and W22 (SRP028545) were divided into gene sets based on their length (1% to 10% represent the shortest set of genes and 91% to 100% represent the longest genes) and the number of genes with insertions in each cds decile, 5′ UTR and 3′ UTR (B73, blue; W22, red).

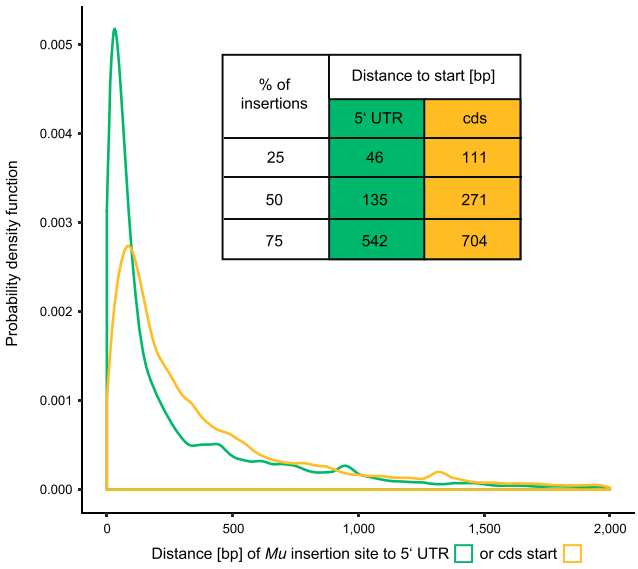

% of insertions	Distance to start [bp]	
	5′ UTR	cds
25	46	111
50	135	271
75	542	704

Figure 5. Distance of *Mu* insertion sites to the start of the 5′ UTR (transcription start site [TSS]) and the cds of affected B73 genes. Density plot illustrating the distances of the *Mu* insertion sites to the 5′ UTR start (green) and the start of the cds (yellow). Only insertion sites located between 500 bp upstream of the 5′ UTR and 2,000 bp downstream of the ATG were considered. Calculated distances of *Mu* insertion sites to the 5′ UTR and the start of affected genes are given in the table.

DISCUSSION

Construction of the European sequence-indexed insertional library (*BonnMu*) in maize discovered 41,086 high quality germinal *Mu* insertions in 16,392 high confidence gene models (Fig. 1), tagging 37% of the B73 genome. This number is comparable with the North American *UniformMu* resource (McCarty et al., 2013; Liu et al., 2016), covering 16,090 genes, which were tagged by 43,943 germinal *Mu* insertions. Recently, an Asian insertional library (*ChinaMu*; Liang et al., 2019) identified 66,565 high-quality germinal insertions representing 20,396 annotated maize genes. In comparison with *UniformMu* and *ChinaMu*, 1,807 genes were newly tagged by *BonnMu*. Hence, with our new European sequence-indexed resource, the percentage of *Mu*-tagged maize genes in public repositories increased from 52% to 57%. Although, this number is still less than that of Arabidopsis (74% of the genes covered; Alonso et al., 2003), it is comparable with rice (about 60% tagged genes; Wang et al., 2013). However it is worth noting that different techniques, such as transfer-DNA insertional mutagenesis (Alonso et al., 2003; Toki et al., 2006), two-component transposon system Ac/Ds based mutagenesis (van Enckevort et al., 2005), or Tos17 retrotransposon mutagenesis (Miyao et al., 2003) were applied to construct insertional libraries in Arabidopsis and rice. Nevertheless, because adequate *Mu*-tagged F_2-families are available in the three global resources (Liang et al., 2019) expanding the datasets is already being implemented to increase the coverage of tagged genes. As described by Liang et al. (2019) we also detected an increase in the number of insertional alleles per gene reducing the efficiency of tagging new genes. A reduction of efficient new gene tagging was also observed in insertional libraries of rice, where more than 246,000 insertions only covered 60% of the genes (Wang et al., 2013). Therefore, our data and previous studies (Kolesnik et al., 2004; Hsing et al., 2007; Zhang, 2007; Liang et al., 2019) suggest that it is difficult, if not impossible, to achieve whole-genome saturation using insertional mutagenesis.

Maize is an excellent model for transposon genetics and mutagenesis studies (Settles et al., 2004). Several endogenous DNA transposon systems, such as *Ac/Ds* (McClintock, 1950) and *Mu* transposons (Robertson, 1978), are highly active in maize and can be easily adopted for large-scale mutagenesis. Genic transposon insertions are usually large enough to cause substantial disruptions of gene function, which are genetically stable (McCarty and Meeley, 2009). Moreover, transposon insertions are relatively easy to identify using molecular genetics and high-throughput sequencing. Nevertheless, early constructed *Mu*-based mutation libraries in maize (Bensen et al., 1995; May et al., 2003; Fernandes et al., 2004) had to deal with (1) inefficient recovery and identification of newly transposed insertions and (2) the challenge to discriminate between germinal and the high background of somatic insertions. Recent studies have overcome both of these challenges. The *Mu*-seq method (McCarty et al., 2013; this study) applies high-throughput NextGen sequencing of *Mu*-tag enriched replicated samples to identify germinal *Mu* insertions. More recently, Liang et al. (2019) achieved *Mu*-tag enrichment utilizing probe hybridization, coupled with high-throughput sequencing to efficiently recover *Mu* insertions in F_2-families of maize. To distinguish germinal from somatic insertions Liang et al. (2019) used a practical criterion (i.e. normalized *Mu*-flanking sequence tag read counts), in addition to the replicated samples as were used for the *UniformMu* analysis (McCarty et al., 2013).

Since the present European *BonnMu* and the North American *UniformMu* insertional library was constructed using the *Mu*-seq approach, *Mu* insertion sites of *BonnMu* were analyzed and compared in more detail with the *UniformMu* library. Due to multiple-round backcrossing between the mutagenic parents and the uniform W22 inbred line, the *UniformMu* lines captured on average five new germinal insertions (McCarty et al., 2005), already excluding about 40 ancestral insertions in the W22 genome (D. R. McCarty, personal communication; Supplemental Dataset S5). However, the *BonnMu* libraries presented here captured 37 germinal insertions in genes of the FGS per F_2-family on average (Supplemental Tables S2 and S3; Supplemental Dataset S3).

For about 50% of the *BonnMu* and *UniformMu*-tagged genes, we observed a gene-size– dependent number of insertions (Fig. 2B; Supplemental Fig. S2). On average, 2.5 insertions were detected per *Mu*-tagged gene, and we observed an association between insertion sites in

B73 and W22 (i.e. hotspots of insertions), which are conserved among tagged genes of both genomes (Fig. 3). The availability of the W22v2 assembly (Springer et al., 2018) allows for comparisons with the B73v4 reference genome at multiple scales, such as *Mu* transposon composition. In total, 75% to 80% of the genes are present at syntenic locations in both maize inbred lines (Springer et al., 2018), making a comparison suitable. To provide additional support for the notion that insertion hotspots are conserved among tagged genes in B73 and W22, it will be essential to analyze and compare a larger W22-*Mu*-seq dataset.

Previous studies revealed that *Mu* insertions concentrate in genomic regions with epigenetic marks of open chromatin near the TSS (Dietrich et al., 2002; Liu et al., 2009; Springer et al., 2018). Indeed, *Mu* elements do exhibit a strong preference for 5′ UTRs of genes (Fig. 4; Dietrich et al., 2002; Liang et al., 2019). Even more precisely, we demonstrated that 50% of all *BonnMu* insertions are located within 135 bp of the TSS (Fig. 5). Pericentromeric regions, which are rich in heterochromatin, display low frequencies of *Mu* insertions and meiotic recombinations (Liu et al., 2009), suggesting an association of site selection for *Mu* insertions with chromatin structure. Indeed, locations for novel transposon insertions can be sensitive to chromatin structure (Naito et al., 2009; Sultana et al., 2017; Springer et al., 2018). For instance, DNA methylation patterns were analyzed by whole-genome bisulfite sequencing and chromatin accessibility throughout the W22 genome using a Micrococcal Nuclease assay (Springer et al., 2018). The enrichment of open chromatin, based on epigenetic marks, such as Cytosin methylation (CHH, where H = A, T, or C) and Micrococcal Nuclease treatment at the TSS and the 3′ UTR of genes (Regulski et al., 2013; Springer et al., 2018) corresponds with the majority of *BonnMu* insertions detected near the 5′ UTR region of genes (Figs. 4 and 5) and a smaller peak near the 3′ UTR (Fig. 4A). Hence, it is likely that chromatin structure plays a key role in site selection for *Mu* insertions. Further indirect support of the hypothesis that open chromatin drives *Mu* insertion sites preferences is shown in Figure 1. The high number of observed *Mu*-tagged genes overlapping among the libraries suggests that the genes are not randomly selected by *Mu*. To further test the hypothesis that open chromatic marks drives *Mu* insertion site preferences, chemical treatment to promote chromatin opening (Baubec et al., 2009) could be applied, thereby facilitating *Mu* insertions in heterochromatic (i.e. inaccessible regions). Another indirect strategy to support this hypothesis is to test if the subset of genes that is not yet *Mu* tagged in any of the published libraries belongs to transcriptionally silenced genes with densely methylated chromatin.

CONCLUSION

In summary, our publicly available European *BonnMu* insertional library provides a starting point for forward and reverse genetics studies in maize. To facilitate functional genomics study in maize, specific mutants and respective phenotypes of segregating F_2-families can be identified based on gene sequences of interest through MaizeGDB.org as described in Liu et al. (2016). Detected on the basis of albino and pale green leaf phenotypes, the mutation rate was ~13%, which is consistent with previously published mutation rates (Robertson, 1983), suggesting a high transposon activity in these stocks. The European *BonnMu* resource is still expanding to archive additional genes tagged by germinal *Mu* insertions. To accelerate the identification of *Mu* insertion sites of future *Mu*-seq libraries, we created a *Mu*-seq workflow utility (*Mu*WU), which is publicly available at https://github.com/Crop-Bioinformatics-Bonn/MuWU. Our *Mu*WU makes use of bioconda (Grüning et al., 2018) and snakemake (Köster and Rahmann, 2012) to provide an easy to install and completely automated framework for the detection and annotation of *Mu* insertion sites.

MATERIAL AND METHODS

Plant Material

The *Mu*-tagged maize (*Zea mays*) F_1-population was generated in the summer season of 2014 by crossing an active *Mu* line (*Mu*[4] per se; Robertson, 1983) into B73 at the experimental field station Campus Klein Altendorf (University of Bonn). The F_1-generation, which is heterozygous for the new *Mu* insertions, was self-pollinated during winter nursery 2014 to 2015 in Chile and in the summer season 2015 at Campus Klein Altendorf to produce segregating F_2-families.

Mu-seq Library Production

For construction of two multiplexed *Mu*-seq libraries we used 1,152 (2×576) F_2-families in the B73 background and followed the previously described *Mu*-seq approach (McCarty et al., 2013). Briefly, each of the two *Mu*-seq libraries contained 576 F_2-families, which were pooled according to a two-dimensional 24×24 grid design (Supplemental Table S1). Hence, the two *Mu*-seq libraries consisted of 1,152 ($2 \times 24 \times 24$) F_2-families. Construction of the *Mu*-seq libraries started with germination of 2×576 maize F_2-families (6 seeds per F_2-family) in paper rolls (Hetz et al., 1996). Sampling of leaf-tissue was carried out 10 to 12 d after germination, according to the 24×24 grid design, where each family contributed to one distinct column and one distinct row pool. In total, there were 24 row and 24 column pools, which created 48 multiplexed leaf samples. Depending on the germination rate, 3 to 6 seedlings were sampled per F_2-family. If less than 3 seedlings germinated, seeds of these F_2-families were regerminated to complement the number of seedlings. A probability was calculated of 99% (Supplemental Table S5) to obtain at least one mutant allele per tagged gene among the 3 to 6 germinated plants per F_2-family. To ensure the specific identification of heritable germinal insertions at intersections of rows and columns in the grid, leaf samples of row and column pools were taken from independent somatic cell lineages, that is, from alternate leaves of each seedling. By utilizing this approach, nonheritable, somatic insertions appeared only in a single axis of the grid and they were excluded from further analyses. Subsequently, gDNA was isolated from these 48 pools (Nalini et al., 2003) and randomly fragmented to a size of about 1 kb using 1 to 3 cycles of 3 min sonication using an Ultrasonication unit followed by 3 min rigorous vortexing. The single stranded overhang of the randomly sheared gDNA fragments was filled in by an enzyme mix to create blunt ends that enabled ligation of a double-stranded universal (U) adapter. Afterward, *Mu*-flanking amplicons were enriched by ligation-mediated PCR using a *Mu*-TIR-specific and a specific primer for the ligated U adapter (PCR I). Two subsequent rounds of PCR (PCR II and III) used nested TIR primers in combination with Illumina sequencing adapter primers to successively incorporate the adapters, necessary for sequencing of the fragments. To reduce the number of very short *Mu*-flanking fragments, PCR II

products were purified to a size range of 300 to 800 bp on 1.2% (w/v) agarose gels. To avoid sample contamination, each of the 48 PCR II products was loaded on a separate gel. The final PCR III completed the required sequencing adapters and incorporated a 6-bp barcode allowing multiplexing of the 48 pools. Finally, each *Mu*-seq library was quantified using a Bioanalyzer, DNA 7500 chip (Agilent Technologies). The final concentrations of the two *Mu*-seq libraries were 73 and 102 nM. Paired-end sequencing (100 bp) of the multiplexed *Mu*-seq libraries was performed in two separate lanes of a HiSeq 2500 (Illumina) sequencer.

Identification of *Mu* Insertion Sites in B73

Adapters and TIR sequences were cut from both ends of the raw *Mu*-seq reads with cutadapt v2.3 (-e 0.2; Martin, 2011). Low-quality bases were filtered with Trimmomatic v0.36 (SLIDINGWINDOW:4:15; MINLEN:12; Bolger et al., 2014) and mapped to the maize reference genome AGPv4.36 (Jiao et al., 2017) with Bowtie2 v2.5.0 (Langmead and Salzberg, 2012). Duplicate reads were removed with the Picard MarkDuplicates tool v2.5.0 (Picard Toolkit, 2019: https://github.com/broadinstitute/picard). *Mu* insertion sites were identified using a customized Python script based on the characteristic 9 bp overlap of *Mu* insertion flanking sequences (McCarty et al., 2013). An insertion site was selected if the 9-bp overlap was supported by at least two reads on each side. To detect insertions that can be assigned to a specific maize F_2-family, all insertion sites with matching genomic coordinates in only one row and one column sample were selected. To identify *Mu* insertion sites inside or upstream of genes of the B73 Filtered Gene Set v4.36 (FGS; Jiao et al., 2017), the Bioconductor R packages IRanges v2.16 and GenomicRanges v1.36 (Lawrence et al., 2013), as well as ChIPpeakAnno v3.16.1 (Zhu et al., 2010) were subsequently used. Only *Mu* insertion sites located inside or upstream (≤500 bp) of FGS genes were considered. The Pearson correlation coefficient was calculated in R v3.5.2 to test the hypothesis that the number of *Mu* insertions increased with the length of the affected genes.

To determine the expected number of FGS genes being *Mu* tagged among *BonnMu* libraries and global sequence-indexed libraries (Fig. 1; Supplemental Table S4), a generalized linear model with a log-link and Poisson distribution was fitted under the assumption of independence between the three available *Mu*-seq resources using *proc genmod* in SAS 9.4 (SAS Institute). For each comparison, the model under independence comprised main effects for each of the compared resources. The expected and observed numbers of *Mu*-tagged FGS genes were compared using a χ^2-test for the two- or three-way interaction effect of the compared resources, respectively. Significant differences were determined at a significance level of $\alpha = 0.05$. Because it was not known which genome versions were used to align the reads of the *UniformMu* or the *ChinaMu* datasets, the reference genome AGPv4.36, used in this study, was applied. Hence, only 16,066 *UniformMu* genes and 20,133 *ChinaMu* genes (Fig. 1B) were considered for the calculation of expected values.

Identification of *Mu* Insertion Sites in W22

Single-end raw *Mu*-seq reads in W22 background (SRA accession SRP028545) were trimmed with cutadapt v2.3 (-e 0.2; Martin, 2011). The barcode and the TIR sequence were cut from the beginning of each read. Reads without TIR sequence were discarded and bases were cut from the end of the remaining reads with Trimmomatic v0.36 (Bolger et al., 2014) if they fell below a quality score of 20 (TRAILING:20; MINLEN:12). Reads were mapped to the maize. reference genome W22 v2.0 (Springer et al., 2018) with Bowtie2 v2.5.0 (Langmead and Salzberg, 2012), and duplicate reads were subsequently removed using the Picard MarkDuplicates tool v2.5.0 (Picard Toolkit, 2019: https://github.com/broadinstitute/picard). Reads that mapped to more than one position were excluded from the deduplicated SAM files and *Mu* insertion sites were identified using a customized Python script. Genomic coordinates were tagged as *Mu* transposon insertion sites if the alignment start of at least two reads matched at the same position. Insertion sites located inside W22 v2.0 genes (Springer et al., 2018) were identified with the R Bioconductor packages IRanges v2.16, GenomicRanges v1.36 (Lawrence et al., 2013), and ChIPpeakAnno v3.16.1 (Zhu et al., 2010), and all insertion sites located inside W22 genes were selected.

Analysis of *Mu* Insertion Sites in B73 and W22

To analyze hotspots of *Mu* insertion sites in B73 and W22, all insertion sites were sorted into corresponding bins. To this end, the length of each gene was divided into bins of 200 bp in size and the number of bins (i.e. hotspots) containing *Mu* transposon insertions was counted for each gene. To compare hotspots between B73 and W22, *Mu* flanking sequences in W22 were extracted (50 bp upstream – 50 bp downstream of the insertion site) using BEDTools v2.25.0 (Quinlan and Hall, 2010) and aligned to the maize. reference genome AGPv4.36 (Jiao et al., 2017) with Bowtie2 v2.5.0 (Langmead and Salzberg, 2012). Multireads (i.e. reads aligning to multiple genomic locations) were excluded and B73 coordinates of W22 reads were further analyzed to identify W22 *Mu* insertion sites within genes of the B73 FGS (Jiao et al., 2017) as described above. Identified insertion sites in W22 and B73 were filtered for endogenous *Mu* elements. To this end, matches between sequences of endogenous *Mu* elements (Springer et al., 2018) and *Mu* insertion flanking sequences (200 bp upstream – 200 bp downstream of the insertion site) were identified with BLAST v2.3.0 (Camacho et al., 2009). Matches that exceeded the defined threshold (pident ≥ 95; bitscore ≥ 50) were excluded from further analyses. Remaining *Mu*-tagged genes that were hit in both B73 and W22 were divided into 200-bp bins. The filtered *Mu* insertions were sorted into the corresponding bins. A χ^2-test ($\alpha \leq 0.01$) was performed on the confusion matrix given in Table 2 in R v3.5.2 to test the hypothesis that there was an association between hotspots in B73 and W22.

To analyze insertion site preferences of *Mu* transposons, the longest transcript for each affected gene in either B73 or W22 was selected and the cds was divided into deciles based on the B73 FGS (Jiao et al., 2017). Genes without annotated cds were excluded from further analyses. All identified insertion sites located in the cds, including endogenous *Mu* elements, were sorted into the corresponding cds decile. Insertion sites located within FGS genes, but up- or downstream of the cds, were counted as an insertion site in the 5′ UTR and 3′ UTR, respectively. To determine the distance from each *Mu* insertion site to the TSS, the longest transcript of each FGS gene was selected. For each *Mu* insertion site identified in B73 inside or upstream (≤500 bp) of B73 FGS genes, the absolute distance to both the cds start and, if available, the 5′ UTR start of the associated gene was calculated.

Accession Numbers

Raw sequencing data are stored at the Sequence Read Archive (http://www.ncbi.nlm.nih.gov/sra) with the accession number PRJNA608624.

Supplemental Data

The following supplemental materials are available.

Supplemental Figure S1. Size distribution of 16,392 affected FGS genes in comparison to the size distribution of all 44,117 B73v4 genes.

Supplemental Figure S2. Number of affected W22 genes and associated number of *Mu* insertions plotted against the corresponding gene size.

Supplemental Figure S3. Number of regions (200 bp bins) in FGS genes preferentially targeted by *Mu* transposons.

Supplemental Figure S4. Affected genes sorted into gene sets according to their length (deciles).

Supplemental Table S1. Grid design for 24 x 24 F_2-families, i.e. 576 F_2-families per *Mu*-seq library.

Supplemental Table S2. Number of germinal *Mu* insertions in FGS genes per 576 F_2-families (*Mu*-seq 1).

Supplemental Table S3. Number of germinal *Mu* insertions in FGS genes per 576 F_2-families (*Mu*-seq 2).

Supplemental Table S4. Number of observed and expected *Mu*-tagged genes among sequence-indexed *Mu* insertional libraries (related to Fig. 1).

Supplemental Table S5. Calculated probability to obtain at least one mutant allele per tagged gene among the 3-6 germinated plants per F_2-family.

Supplemental Dataset S1. Number of raw read pairs per row and column sample sequenced per *Mu*-seq library with HiSeq2500 (Illumina) sequencer.

Supplemental Dataset S2. A total of 225,936 genomic insertion sites detected in the two *Mu*-seq libraries.

Supplemental Dataset S3. A total of 41,086 *Mu* insertion sites detected in 16,392 genes of the FGS.

Supplemental Dataset S4. List of 43,943 *UniformMu* insertions within 16,090 genes in B73.

Supplemental Dataset S5. Canonical *Mu* elements in W22 and B73.

ACKNOWLEDGMENTS

We thank Hans-Peter Piepho (University of Hohenheim) for statistical assistance and Patrick S. Schnable (Iowa State University) for providing seeds of Mu^4 per se. We also appreciate the help of Peng Yu (University of Bonn) in this project. We thank Karl-Josef Wiesel (Campus Klein Altendorf, University of Bonn), Christa Schulz, and Helmut Rehkopf (University of Bonn) for technical assistance.

Received April 20, 2020; accepted July 27, 2020; published August 7, 2020.

LITERATURE CITED

Alonso JM, Stepanova AN, Leisse TJ, Kim CJ, Chen H, Shinn P, Stevenson DK, Zimmerman J, Barajas P, Cheuk R, et al (2003) Genome-wide insertional mutagenesis of *Arabidopsis thaliana*. Science **301:** 653–657

Baubec T, Pecinka A, Rozhon W, Mittelsten Scheid O (2009) Effective, homogeneous and transient interference with cytosine methylation in plant genomic DNA by zebularine. Plant J **57:** 542–554

Bennetzen JL (2000) Transposable element contributions to plant gene and genome evolution. Plant Mol Biol **42:** 251–269

Bensen RJ, Johal GS, Crane VC, Tossberg JT, Schnable PS, Meeley RB, Briggs SP (1995) Cloning and characterization of the maize *An1* gene. Plant Cell **7:** 75–84

Bolger AM, Lohse M, Usadel B (2014) Trimmomatic: A flexible trimmer for Illumina sequence data. Bioinformatics **30:** 2114–2120

Brutnell TP (2002) Transposon tagging in maize. Funct Integr Genomics **2:** 4–12

Camacho C, Coulouris G, Avagyan V, Ma N, Papadopoulos J, Bealer K, Madden TL (2009) BLAST+: Architecture and applications. BMC Bioinformatics **10:** 421

Candela H, Hake S (2008) The art and design of genetic screens: maize. Nat Rev Genet **9:** 192–203

Chandler VL, Hardeman KJ (1992) The *Mu* elements of *Zea mays*. Adv Genet **30:** 77–122

Dietrich CR, Cui F, Packila ML, Li J, Ashlock DA, Nikolau BJ, Schnable PS (2002) Maize *Mu* transposons are targeted to the 5′ untranslated region of the *gl8* gene and sequences flanking *Mu* target-site duplications exhibit nonrandom nucleotide composition throughout the genome. Genetics **160:** 697–716

Fernandes J, Dong Q, Schneider B, Morrow DJ, Nan GL, Brendel V, Walbot V (2004) Genome-wide mutagenesis of *Zea mays* L. using RescueMu transposons. Genome Biol **5:** R82

Feschotte C, Jiang N, Wessler SR (2002) Plant transposable elements: Where genetics meets genomics. Nat Rev Genet **3:** 329–341

Frey M, Stettner C, Gierl A (1998) A general method for gene isolation in tagging approaches: Amplification of insertion mutagenised sites (AIMS). Plant J **13:** 717–721

Grüning B, Dale R, Sjödin A, Chapman BA, Rowe J, Tomkins-Tinch CH, Valieris R, Köster J; Bioconda Team (2018) Bioconda: Sustainable and comprehensive software distribution for the life sciences. Nat Methods **15:** 475–476

Hetz W, Hochholdinger F, Schwall M, Feix G (1996) Isolation and characterization of *rtcs*, a maize mutant deficient in the formation of nodal roots. Plant J **10:** 845–857

Hirochika H, Guiderdoni E, An G, Hsing YI, Eun MY, Han CD, Upadhyaya N, Ramachandran S, Zhang Q, Pereira A, et al (2004) Rice mutant resources for gene discovery. Plant Mol Biol **54:** 325–334

Hochholdinger F, Wen TJ, Zimmermann R, Chimot-Marolle P, da Costa e Silva O, Bruce W, Lamkey KR, Wienand U, Schnable PS (2008) The maize (*Zea mays* L.) *roothairless3* gene encodes a putative GPI-anchored, monocot-specific, COBRA-like protein that significantly affects grain yield. Plant J **54:** 888–898

Hsing YI, Chern CG, Fan MJ, Lu PC, Chen KT, Lo SF, Sun PK, Ho SL, Lee KW, Wang YC, et al (2007) A rice gene activation/knockout mutant resource for high throughput functional genomics. Plant Mol Biol **63:** 351–364

Jiao Y, Peluso P, Shi J, Liang T, Stitzer MC, Wang B, Campbell MS, Stein JC, Wei X, Chin CS, et al (2017) Improved maize reference genome with single-molecule technologies. Nature **546:** 524–527

Kolesnik T, Szeverenyi I, Bachmann D, Kumar CS, Jiang S, Ramamoorthy R, Cai M, Ma ZG, Sundaresan V, Ramachandran S (2004) Establishing an efficient Ac/Ds tagging system in rice: Large-scale analysis of Ds flanking sequences. Plant J **37:** 301–314

Köster J, Rahmann S (2012) Snakemake--a scalable bioinformatics workflow engine. Bioinformatics **28:** 2520–2522

Langmead B, Salzberg SL (2012) Fast gapped-read alignment with Bowtie 2. Nat Methods **9:** 357–359

Lawrence M, Huber W, Pagès H, Aboyoun P, Carlson M, Gentleman R, Morgan MT, Carey VJ (2013) Software for computing and annotating genomic ranges. PLOS Comput Biol **9:** e1003118

Liang L, Zhou L, Tang Y, Li N, Song T, Shao W, Zhang Z, Cai P, Feng F, Ma Y, et al (2019) A sequence-indexed *Mutator* insertional library for maize functional genomics study. Plant Physiol **181:** 1404–1414

Lisch D (2002) *Mutator* transposons. Trends Plant Sci **7:** 498–504

Lisch D (2015) Mutator and MULE transposons. Microbiol Spectr **3:** MDNA3-0032-2014

Liu P, McCarty DR, Koch KE (2016) Transposon mutagenesis and analysis of mutants in *UniformMu* maize (*Zea mays*). Curr Protoc Plant Biol **1:** 451–465

Liu S, Yeh CT, Ji T, Ying K, Wu H, Tang HM, Fu Y, Nettleton D, Schnable PS (2009) *Mu* transposon insertion sites and meiotic recombination events co-localize with epigenetic marks for open chromatin across the maize genome. PLoS Genet **5:** e1000733

Liu YG, Whittier RF (1995) Thermal asymmetric interlaced PCR: Automatable amplification and sequencing of insert end fragments from P1 and YAC clones for chromosome walking. Genomics **25:** 674–681

Martin M (2011) Cutadapt removes adapter sequences from high-throughput sequencing reads. EMBnet J **17:** 10–12

May BP, Liu H, Vollbrecht E, Senior L, Rabinowicz PD, Roh D, Pan X, Stein L, Freeling M, Alexander D, et al (2003) Maize-targeted mutagenesis: A knockout resource for maize. Proc Natl Acad Sci USA **100:** 11541–11546

McCarty DR, Latshaw S, Wu S, Suzuki M, Hunter CT, Avigne WT, Koch KE (2013) Mu-seq: Sequence-based mapping and identification of transposon induced mutations. PLoS One **8:** e77172

McCarty DR, Meeley RB (2009) Transposon resources for forward and reverse genetics in maize. In J.L. Bennetzen, and S. Hake, eds, Handbook of Maize. Springer, New York, pp 561–584

McCarty DR, Settles AM, Suzuki M, Tan BC, Latshaw S, Porch T, Robin K, Baier J, Avigne W, Lai J, et al (2005) Steady-state transposon mutagenesis in inbred maize. Plant J **44:** 52–61

McClintock B (1950) The origin and behavior of mutable loci in maize. Proc Natl Acad Sci USA **36:** 344–355

McClintock B (1951) Mutable loci in maize. Carnegie Institution of Washington Yearbook **50:** 174–181

Miyao A, Tanaka K, Murata K, Sawaki H, Takeda S, Abe K, Shinozuka Y, Onosato K, Hirochika H (2003) Target site specificity of the Tos17 retrotransposon shows a preference for insertion within genes and against insertion in retrotransposon-rich regions of the genome. Plant Cell **15:** 1771–1780

Naito K, Zhang F, Tsukiyama T, Saito H, Hancock CN, Richardson AO, Okumoto Y, Tanisaka T, Wessler SR (2009) Unexpected consequences of a sudden and massive transposon amplification on rice gene expression. Nature **461:** 1130–1134

Nalini E, Bhagwat SG, Jawali N (2003) A simple method for isolation of DNA from plants suitable for long term storage and DNA marker analysis. BARC Newsletter **249:** 208–214

Nestler J, Liu S, Wen TJ, Paschold A, Marcon C, Tang HM, Li D, Li L, Meeley RB, Sakai H, et al (2014) *Roothairless5*, which functions in maize (*Zea mays* L.) root hair initiation and elongation encodes a monocot-specific NADPH oxidase. Plant J **79:** 729–740

Portwood JL II, Woodhouse MR, Cannon EK, Gardiner JM, Harper LC, Schaeffer ML, Walsh JR, Sen TZ, Cho KT, Schott DA, et al (2019) MaizeGDB 2018: The maize multi-genome genetics and genomics database. Nucleic Acids Res **47**(D1): D1146–D1154

Quinlan AR, Hall IM (2010) BEDTools: A flexible suite of utilities for comparing genomic features. Bioinformatics **26:** 841–842

Regulski M, Lu Z, Kendall J, Donoghue MTA, Reinders J, Llaca V, Deschamps S, Smith A, Levy D, McCombie WR, et al (2013) The maize methylome influences mRNA splice sites and reveals widespread paramutation-like switches guided by small RNA. Genome Res **23:** 1651–1662

Robertson DS (1978) Characterization of a *mutator* system in maize. Mutat Res **51:** 21–28

Robertson DS (1983) A possible dose-dependent inactivation of *Mutator* (*Mu*) in maize. Mol Gen Genet **191:** 86–90

Schnable JC, Freeling M (2011) Genes identified by visible mutant phenotypes show increased bias toward one of two subgenomes of maize. PLoS One **6:** e17855

Schnable PS, Ware D, Fulton RS, Stein JC, Wei F, Pasternak S, Liang C, Zhang J, Fulton L, Graves TA, et al (2009) The B73 maize genome: complexity, diversity, and dynamics. Science **326:** 1112–1115

Settles AM, Latshaw S, McCarty DR (2004) Molecular analysis of high-copy insertion sites in maize. Nucleic Acids Res **32:** e54

Springer NM, Anderson SN, Andorf CM, Ahern KR, Bai F, Barad O, Barbazuk WB, Bass HW, Baruch K, Ben-Zvi G, et al (2018) The maize W22 genome provides a foundation for functional genomics and transposon biology. Nat Genet **50:** 1282–1288

Stern DB, Hanson MR, Barkan A (2004) Genetics and genomics of chloroplast biogenesis: Maize as a model system. Trends Plant Sci **9:** 293–301

Sultana T, Zamborlini A, Cristofari G, Lesage P (2017) Integration site selection by retroviruses and transposable elements in eukaryotes. Nat Rev Genet **18:** 292–308

Toki S, Hara N, Ono K, Onodera H, Tagiri A, Oka S, Tanaka H (2006) Early infection of scutellum tissue with Agrobacterium allows high-speed transformation of rice. Plant J **47:** 969–976

van Enckevort LJ, Droc G, Piffanelli P, Greco R, Gagneur C, Weber C, González VM, Cabot P, Fornara F, Berri S, et al (2005) EU-OSTID: A collection of transposon insertional mutants for functional genomics in rice. Plant Mol Biol **59:** 99–110

Wang N, Long T, Yao W, Xiong L, Zhang Q, Wu C (2013) Mutant resources for the functional analysis of the rice genome. Mol Plant **6:** 596–604

Xu C, Tai H, Saleem M, Ludwig Y, Majer C, Berendzen KW, Nagel KA, Wojciechowski T, Meeley RB, Taramino G, et al (2015) Cooperative action of the paralogous maize lateral organ boundaries (LOB) domain proteins RTCS and RTCL in shoot-borne root formation. New Phytol **207:** 1123–1133

Zhang Q (2007) Strategies for developing green super rice. Proc Natl Acad Sci USA **104:** 16402–16409

Zhu LJ, Gazin C, Lawson ND, Pagès H, Lin SM, Lapointe DS, Green MR (2010) ChIPpeakAnno: A bioconductor package to annotate ChIP-seq and ChIP-chip data. BMC Bioinformatics **11:** 237